Bifurcations at the Eckhaus points in two-dimensional Rayleigh-Bénard convection

M. Nagata
School of Mathematics and Statistics, The University of Birmingham, Edgbaston, Birmingham B15 2TT United Kingdom
(Received 26 April 1994; revised manuscript received 31 March 1995)

A twofold nonlinear solution branch with the fundamental wave number outside the neutral curve is found numerically to connect two Eckhaus points in two-dimensional Rayleigh-Bénard convection. It results from the nonlinear interaction of the primary modes whose wave numbers are in the ratio of 3:5.

PACS number(s): 47.27.Te, 03.40.Gc, 47.20.Ky

Because of its simple configurations, Rayleigh-Bénard convection has been studied most extensively in fluid mechanics as a testing ground for comparison between theory and experimental observations. The nonuniqueness of two-dimensional finite-amplitude convection has been reported by many [1–3], and we are particularly interested in clarifying the bifurcation structure of those solutions that bifurcate at the Eckhaus instability points [4]. So far, mixed-mode solutions with a long wavelength are known to bifurcate at an Eckhaus instability point, but the connection between the mixed-mode solutions was not clear. By restricting nonlinear interactions to odd wave number modes, we find that *two* solutions bifurcate subharmonically at one Eckhuas point at a wave number larger than the critical wave number α_c, and that they terminate simultaneously on another Eckhaus point at a wave number smaller than α_c. We will also discuss the region outside the neutral curve, where the double solution branch exists.

The nondimensional stream function ψ and the temperature deviation θ from the conductive state in two-dimensional Rayleigh-Bénard convection are described by the equations

$$\partial_t \nabla^2\psi + J(\psi,\nabla^2\psi) = \mathrm{Pr}(R\,\partial_x\theta + \nabla^4\psi)\ , \tag{1}$$

$$\partial_t\theta + J(\psi,\theta) = \partial_x\psi + \nabla^2\theta\ , \tag{2}$$

where $J(\ ,\ )$ is the Jacobian, R is the Rayleigh number, and Pr is the Prandtl number. The no-slip condition and fixed temperatures are prescribed on the horizontal boundaries of infinite extent at $z=\pm\frac{1}{2}$:

$$\psi=\partial_z\psi=\theta=0\ . \tag{3}$$

Assuming a steady state and a periodicity in the horizontal direction x with wave number α, we expand ψ and θ in the form

$$\psi=\sum_{l=1}^{\infty}\sum_{m=-\infty}^{\infty} a_{lm}\exp(im\alpha x)f_l(z)\ , \tag{4}$$

$$\theta=\sum_{l=1}^{\infty}\sum_{m=-\infty}^{\infty} b_{lm}\exp(im\alpha x)\sin l\pi\left(z+\tfrac{1}{2}\right)\ , \tag{5}$$

where $f_l(z)$ is the Chandrasekhar function [5] satisfying $f_l\ (\pm\frac{1}{2})=f_l'\ (\pm\frac{1}{2})=0$ and is an even (odd) function depending on l being an odd (even) integer. A simple inspection of the basic equations (1) and (2) with the symmetric boundary conditions (3) reveals that among the entire set of modes whose complex amplitudes are a_{lm} and b_{lm}, with l and m being any integers, modes in a subset with

$$l+m=(\text{even integers}) \tag{6}$$

are closed with respect to their nonlinear interactions. We use the symmetry (6) throughout.

For numerical purposes we truncate the expansions (4) and (5) so that only those terms satisfying

$$l+|m|<N_T \tag{7}$$

are taken into account in a Galerkin method.

It is well known that the critical Rayleigh number R_c is 1708 at $\alpha_c=3.116$, irrespective of the Prandtl number [6]. A line of $R=$const above R_c intersects the neutral curve twice, at $\alpha=\alpha_-$ ($<\alpha_c$) and at $\alpha=\alpha_+$ ($>\alpha_c$). In the following computations, Pr=1 is chosen. It is worthwhile mentioning that the two-dimensional roll solutions of Bénard convection with Pr=1 are mathematically identical to the axisymmetric Taylor vortex flows in a narrow gap between two concentric cylinders that rotate with almost equal angular velocities in the same direction [7]. Therefore, our findings are directly applicable to the axisymmetric Taylor vortex flow in the special limit mentioned above [8].

Figure 1 plots the Nusselt number

$$\mathrm{Nu}=1+\sum_l b_{l0}\,l\pi\cos l\pi \tag{8}$$

of the finite amplitude convection at $R=17\,500$. The deviation of the Nusselt number from 1 is a measure of nonlinearity: conductive heat transport corresponds to Nu=1. We follow the main branch from point S in Fig. 1 which is on the neutral curve at $\alpha=\alpha_+$ in the α-R plane. The maximum heat transport takes place at point A near $\alpha=3.0$. As α is decreased further, the branch produces a turning point at T. Passing through B at $\alpha=3.0$ it reaches point P, where amplitudes of all the modes except those with the wave numbers $3M\alpha$ ($M=1,2,\ldots,$) vanish. The modes in this subset are identical to those that constitute the finite amplitude solution on the main branch if 3α is regarded as the fundamental wave number. Mizushima and Fujimura [3] have investigated the bifurcation structure in the neigh-

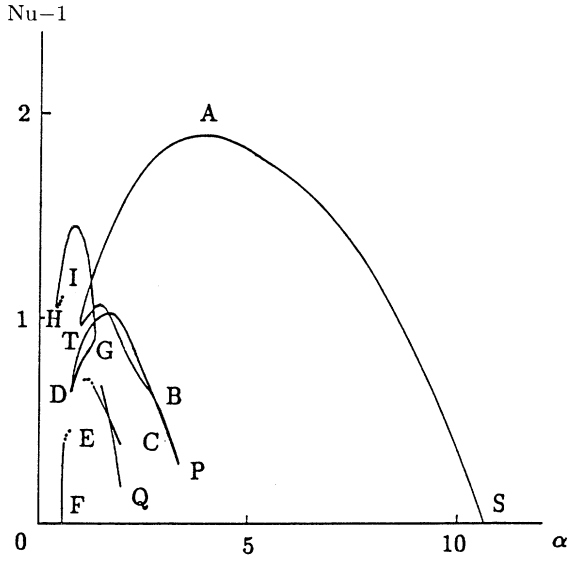

FIG. 1. Nonuniqueness of the two-dimensional Rayleigh-Bénard convection at $R=17\,500$ with $\mathrm{Pr}=1$. The solutions on the G and H and H and I arcs are analyzed. The dots indicate that the segments continue.

borhood of P by considering two primary modes in resonance with the wave number ratio of 1:3. At P the system sheds another 1:3 resonance branch, as in Mizushima and Fujimura [3]. Point C at $\alpha=3.0$ is on this branch. In contrast to the findings of Mizushima and Fujimura, where calculations are carried out for a smaller R with $\mathrm{Pr}=7$, our curve does not reach point F on the neutral curve at $\alpha=\alpha_-$ directly. Instead, the branch undergoes the second turning point D and flips over at G near $\alpha=1.5$, toward a smaller wave number region. After making a small arc, the curve undergoes a third turning point at H and begins to form another arc H and I. It continues to exhibit such a complicated structure that only a few segments of the branch are drawn in Fig. 1. In fact, more than ten different steady states are detected at $\alpha=1.0$. Among the segments drawn in Fig. 1, the F and E segments originate from the point on the neutral curve and the segments (there are two but they are not resolved in the figure) convergent to point Q manifest a 1:5 resonance. Note that the turning point H indicates the existence of fully developed two-dimensional solutions outside the neutral point F. The truncation level in Fig. 1 is $N_T=14$, which one might think is rather small for the Rayleigh number $R\simeq 10.2R_c$. The main feature of the branch, however, does not change even if the truncation number N_T is increased to as much as 24.

In an attempt to extract a simple structure, R is decreased gradually without losing the G and H and H and I arcs. It is found that at $R=3000$ the arcs are already isolated from the main branch, forming an eyebrowlike shape with not only the left ends of the arcs but also the right ends (corresponding to G and I in Fig. 1) connected, as shown in Fig. 2. As the smaller and the larger wave numbers end where the upper and lower arcs meet, all the modes except those whose wave numbers are $3M\alpha$ and $5M\alpha$ ($M=1,2,\ldots,$), respectively, vanish. They correspond to the solutions on the main branch with wave numbers 3α and 5α, respectively. The dent at P on the main branch for $R=3000$ in Fig. 2 results from the 1:3 resonance studied by Mizushima and Fujimura [3]. The 1:5 resonance has not been detected on the main branch at $R=3000$ or less. However, we could not exclude the possibility of isolated 1:5 resonance branches.

In Fig. 2 the arcs have contracted to almost a point, as we can see, at the wave number $\alpha\simeq 0.8$ for $R=1900$. At this Rayleigh number, the modes with wave numbers $3\alpha\simeq 2.4$ and $5\alpha\simeq 4.0$ are almost on the neutral curve at $\alpha=\alpha_-$ and $\alpha=\alpha_+$. Therefore, it seems that the origin of the solutions on the arcs outside the neutral points is due to a 3:5 interaction.

In order to confirm the 3:5 interaction, stability of the main branch with respect to two-dimensional perturbations is examined. The instability due to two-dimensional perturbations is often called the Eckhaus instability. Two-dimensional subharmonic instabilities are of our particular interest. We superpose two-dimensional per-

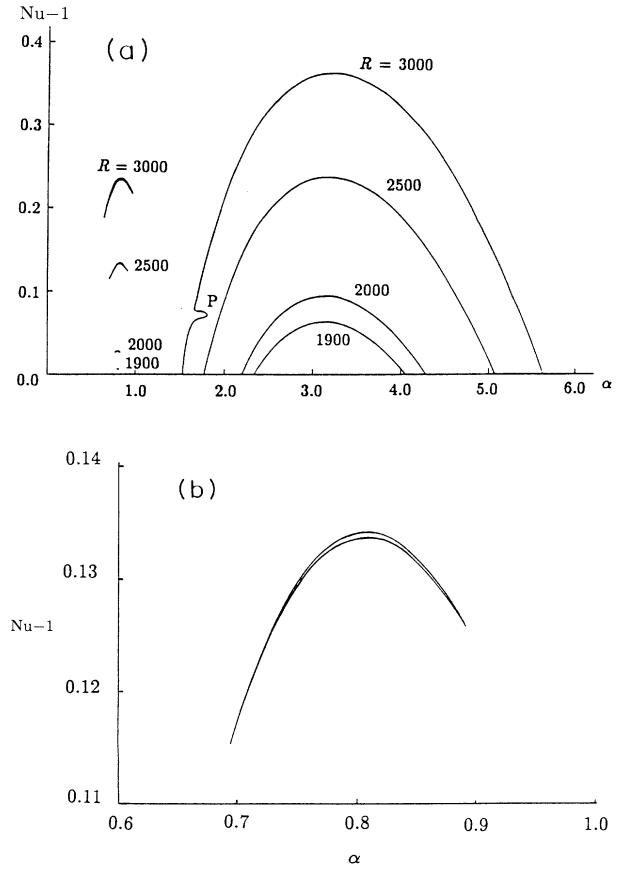

FIG. 2. (a) The two-dimensional solutions isolated from the main branch. The isolated solutions are on two arcs with their end points in common for each R, as exemplified in (b): $R=2500$.

turbations in the form

$$\tilde{\psi}=\sum_{l=1}^{L}\sum_{m=-M}^{M}\tilde{a}_{lm}\exp(im\alpha x)f_l(z)\exp(idx+\sigma t)\ , \tag{9}$$

$$\tilde{\theta}=\sum_{l=1}^{L}\sum_{m=-M}^{M}\tilde{b}_{lm}\exp(im\alpha x)\sin l\pi(z+\tfrac{1}{2})\times\exp(idx+\sigma t) \tag{10}$$

on the finite-amplitude solutions (4) and (5), substitute $\psi+\tilde{\psi}$ and $\theta+\tilde{\theta}$ into Eqs. (1) and (2), linearize the system with respect to perturbations, and solve a resulting eigenvalue problem with the growth rate σ as the eigenvalue for a fixed Floquet parameter d.

Figure 3 shows the growth rate σ of the two-dimensional perturbations (9) and (10) when d is set at an anticipated fraction of α, namely, $d=\frac{1}{3}\alpha$, $\frac{1}{5}\alpha$, and $\frac{2}{5}\alpha$ at various Rayleigh numbers. It can be shown that the perturbation with $d=\frac{2}{3}\alpha$ produces the same set of eigenvalues as the perturbation with $d=\frac{1}{3}\alpha$ does. As R increases from R_c, the sign of the eigenvalue associated with the perturbation with $d=\frac{1}{5}\alpha$ changes from negative to positive values on the larger wave number branch of the neutral curve. Then, the perturbation with $d=\frac{1}{3}\alpha$ becomes critical on the smaller wave number branch of the neutral curve between $R=1760$ and 1800. At $R\simeq 1875$, perturbations with $d=\frac{2}{5}\alpha$ and perturbations with $d=\frac{1}{3}\alpha$ become critical simultaneously on the larger wave number branch of the neutral curve and on the smaller wave number branch of the neutral curve, respectively. These subharmonic bifurcation points are traced in their higher Rayleigh number region inside the neutral curve in Fig. 4.

The curves of the subharmonic bifurcation with $d=\frac{1}{5}\alpha$ and $d=\frac{1}{3}\alpha$ intersect the neutral curve where $\alpha_-:\alpha_+=4:5$ and $\alpha_-:\alpha_+=3:4$, respectively. The subharmonic bifurcations with $d=\frac{1}{3}\alpha$ and $d=\frac{2}{5}\alpha$ occur simultaneously on the neutral curve at $R\simeq 1875$, where $\alpha_-:\alpha_+=3:5$. The weakly nonlinear theory [9] shows that for a two-dimensional solution at $\alpha=k$ near the neutral curve, i.e., $k\simeq\alpha_-$ or $k\simeq\alpha_+$, with R slightly larger than R_c, a pair of perturbations with k_1 and k_2, which satisfy the resonance condition $2k=k_1+k_2$, is responsible for the Eckhaus instability when $k-k_1\simeq\alpha_+-\alpha_-$ or $k_2-k\simeq\alpha_+-\alpha_1$. This result also applies to our strongly nonlinear analysis: Choose $m=-1$ and $m=1$ in $(m+\frac{1}{5})\alpha$ and $(m+\frac{1}{3})\alpha$ to get $\alpha_-:\alpha_+=4:5$ and 3:4, respectively. For simultaneous bifurcation at $\alpha_-:\alpha_+3:5$, set $m=-1$ and $m=-2$ in $(m+\frac{2}{5})\alpha$ and $(m+\frac{1}{3})\alpha$.

When the neutral curve and the bifurcation curves are

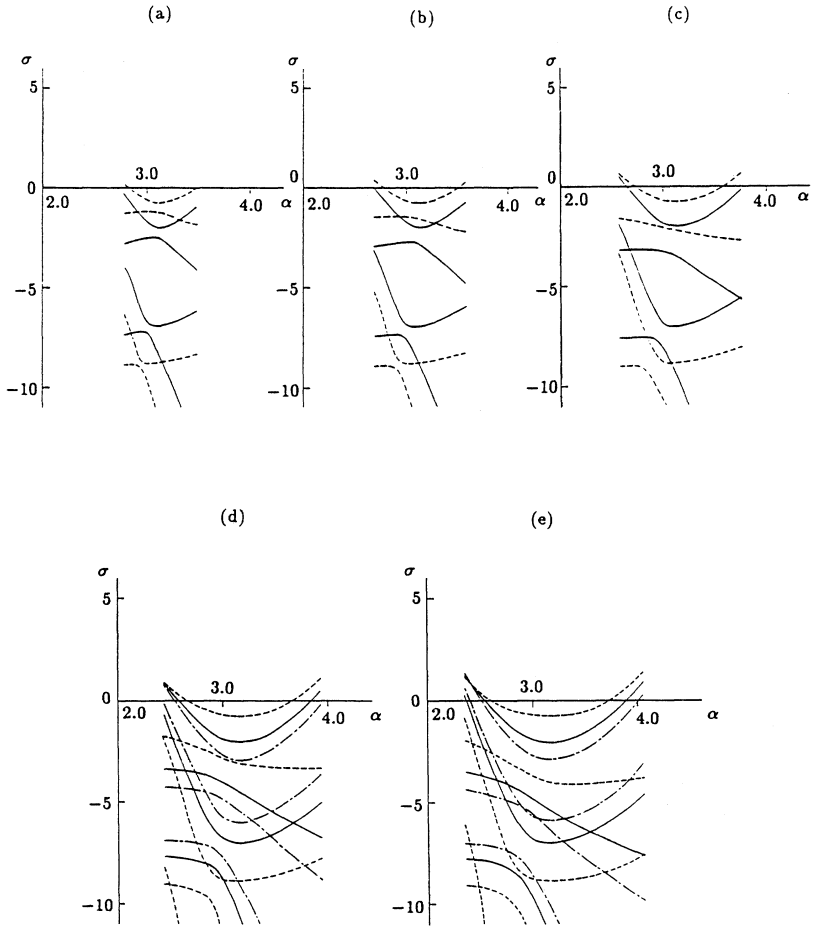

FIG. 3. The growth rates σ as a function of the wave number α of the main branch solution. (a) $R=1740$, (b) $R=1760$, (c) $R=1800$, (d) $R=1850$, (e) $R=1900$. The solid, dashed, and dash-dotted curves indicate a few of the highest growth rates of perturbations with $d=\frac{1}{3}\alpha$, $d=\frac{1}{5}\alpha$, and $d=\frac{2}{5}\alpha$, respectively.

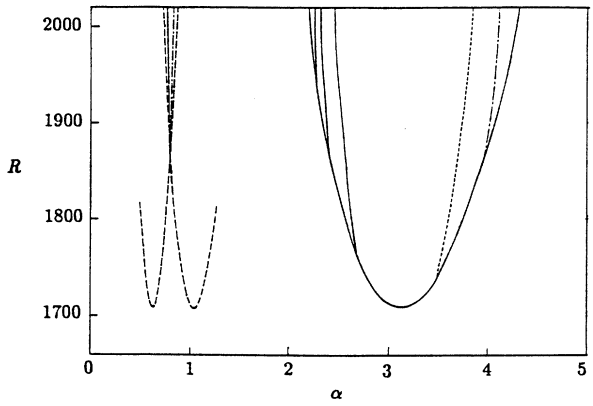

FIG. 4. The subharmonic bifurcation curves inside the neutral curve. On the solid, dashed, and dash-dotted curves, the growth rate of perturbations with $d=\frac{1}{3}\alpha$, $d=\frac{1}{5}\alpha$, and $d=\frac{2}{5}\alpha$, respectively, is zero. The long dashed curves on the left-hand side of the figure are the neutral curves compressed by a third and a fifth in the wave number α.

compressed by 1/3 and 1/5 in wave number α, as is shown on the left-hand side of Fig. 4, one can notice that two bifurcation curves corresponding to $d=\frac{1}{3}\alpha$ and $d=\frac{2}{5}\alpha$ start from the point where the two compressed neutral curves intersect. In the outer cusp region where the two compressed neutral curves overlap, the conventional supercritical finite amplitude solutions on the main branch can be represented by the fundamental mode with the wave number 3α or 5α and the harmonics with the wave number $3M\alpha$ or $5M\alpha$ ($M=2,3,\ldots$) depending on the type of compression. The solution on the arcs outside the neutral curve bifurcates from the Eckhaus points on the main branch for $d=\frac{2}{5}\alpha$ at the right edge of the arcs and for $d=\frac{1}{3}\alpha$ at the left edge of the arcs (see Fig. 5). The solutions on the arcs exist in the inner cusp region bounded by these two Eckhaus instability points in Fig. 4. Although the Nusselt numbers of the solutions on the two arcs are almost identical, as we can see in Fig. 5, their convective patterns are quite different, as can be seen in Fig. 6. On one branch, a roll whose rotation is opposite to the neighboring two rolls is elongated until it is halved, and a roll with a different rotation squeezes into the gap between the bisected roll as the wave number is increased [see Figs. 6(a)–6(e)]. On the other branch, three rolls are squashed in a group, and a pair of rolls with different rotations fits the gap [see Figs. 6(f)–6(j)].

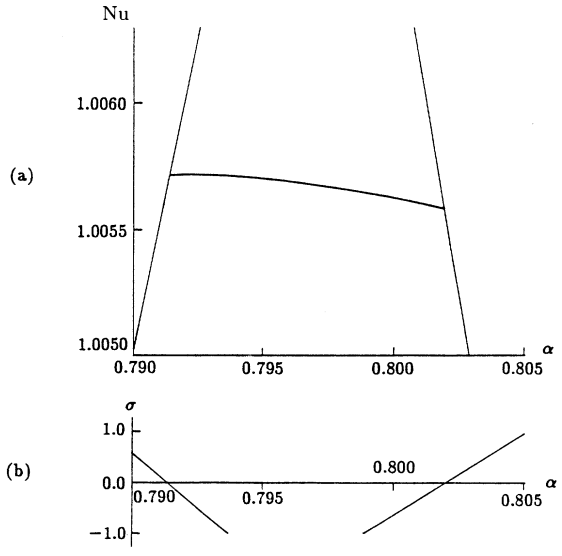

FIG. 5. (a) Two solution branches (thick curves hardly distinguishable from each other in terms of the Nusselt number) connecting the compressed main branches (thin curves). The main branch solution of the right is composed of modes whose wave numbers are $5M\alpha$ ($M=1,2,\ldots,$), whereas modes with $3M\alpha$ ($M=1,2,\ldots,$) constitute a main branch solution on the left. $R=1900$. (b) The growth rate σ of the perturbations with $d=\frac{1}{3}\alpha$ for a smaller α and $d=\frac{2}{5}\alpha$ for a larger α on the compressed main branch.

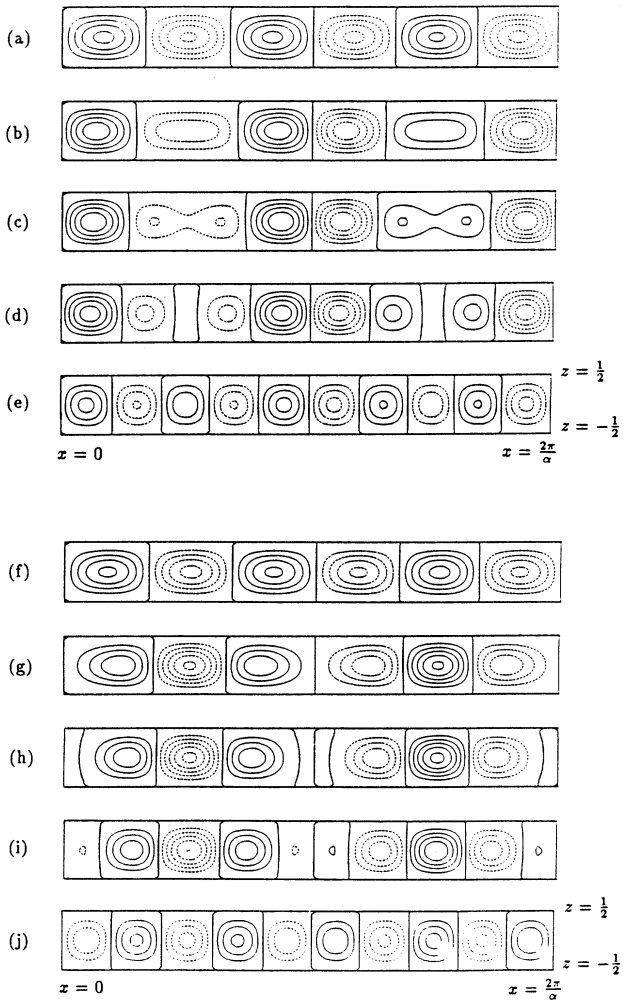

FIG. 6. The stream functions on the upper branch, (a), (b), (c), (d), (e), and the lower branch, (f), (g), (h), (i), (j). $R=1900$. In (a), (f), $\alpha=0.7914$; in (b), (g), $\alpha=0.793$; in (c), (h), $\alpha=0.796$; in (d), (i), $\alpha=0.799$; in (e), (j), $\alpha=0.8019$.

The evolution of the solution near the vertex of the cusps in Fig. 4 can be analyzed by using an amplitude expansion method or a normal form analysis similar to the study by Knobloch and Guckenheimer [1], who examined the k:$(k+1)$ interaction in the two-dimensional convection with the stress free boundary condition. Since their primary modes, the k mode and the $(k+1)$ mode, are symmetric in z, the 1 mode (the "slave mode") is antisymmetric in z through the quadratic interaction of the primary modes. The difference between their case and our case is that our case demonstrates the interaction within the subset associated with the symmetry $(l+m)$:(even) so that the fundamental mode (the 1 mode) still retains the same symmetry as the primary modes (the 3 mode and the 5 mode). Even modes created by the interaction of the 3 mode and the 5 mode are antisymmetric in z. Ensuing interactions between the even modes and the primary modes produce the fundamental mode, which is symmetric in z. Therefore, one can deduce that the primary mode would be governed by a pair of fifth order evolution equations in the 3:5 interaction. Third order coupled evolution equations cannot resolve the double structure of the solution branch. The solutions can exist in the absence of the modes with $(l+m)$:(odd). A detailed analysis using the amplitude expansion based on the center manifold theory will follow in a separate paper.

The stability of the solutions against general three-dimensional perturbations should be examined. Tuckerman and Barkley [4] showed that the solutions bifurcating from the Eckhaus points are unstable with respect to two-dimensional perturbations. The Taylor vortex version of the solution may explain the braided vortices observed experimentally [10] if it gives rise to a stable three-dimensional structure at a higher Taylor number. The braided vortex flow is characterized by a large number of vortex boundary dislocations and can be produced only through a sudden change in the rotation speed of the concentric cylinders. We emphasize that stability properties are different between the Taylor-Couette system and the Bénard convection since the mathematical identity between the two problems ceases to hold for three-dimensional flows. Other cases with $\mathrm{Pr} \neq 1$ must also be investigated. In general, one could expect $(2k-1)$:$(2k+1)$ interactions to occur, although those with $k \geq 3$ would be weaker.

[1] E. Knobloch and J. Guckenhmeier, Phys. Rev. A **27**, 408 (1983).

[2] F. H. Busse and A. C. Or, Z. Angew. Math. Phys. **37**, 608 (1986); F. H. Busse, in *Bifurcation: Analysis, Algorithms, Applications,* edited by T. Küpper, R. Seydel, and H. Troger (Birkhäuser, Verlag Basel, 1987), Vol. 79, p. 18; C. A. Jones and M. R. E. Proctor, Phys. Lett. A **121**, 224 (1987); J. Mizushima, Fluid Dyn. Res. **11**, 297 (1993).

[3] J. Mizushima and K. Fujimura, J. Fluid Mech. **234**, 651 (1992).

[4] L. Kramer and W. Zimmermann, Physica **16D**, 221 (1985); L. S. Tuckerman and D. Barkley, Physica **46D**, 57 (1990).

[5] S. Chandrasekhar, *Hydrodynamic and Hydromagnetic Stability* (Oxford University, Oxford, 1961).

[6] P. G. Drazin and W. H. Reid, *Hydrodynamic Stability* (Cambridge University, Cambridge, 1981).

[7] M. Nagata, J. Fluid Mech. **169**, 229 (1986).

[8] The nonuniqueness of axisymmetric Taylor vortex flows has been demonstrated in the following papers: G. Frank and R. Mayer-Spasche, Z. Angew. Math. Phys. **32**, 710 (1981); R. Mayer-Spasche and H. B. Keller, Phys. Fluids **28**, 1248 (1985); H. Specht, M. Wagner, and R. Mayer-Spasche, Z. Angew. Math. Mech. **69**, 339 (1989).

[9] W. Eckhaus, in *Studies in Nonlinear Stability Theory* (Springer, New York, 1976); J. T. Stuart and R. C. DiPrima, Proc. R. Soc. London, A **362**, 27 (1978).

[10] D. C. Andereck, R. Dickman, and H. L. Swinney, Phys. Fluids **26**, 1395 (1983); D. C. Andereck, S. S. Liu, and H. L. Swinney, J. Fluid Mech. **164**, 155 (1986).